Protein Science (1999), *8*:84–90. Cambridge University Press. Printed in the USA.

Crystal structure of a designed, thermostable, heterotrimeric coiled coil

SHIVANI NAUTIYAL AND TOM ALBER

Department of Molecular and Cell Biology, 229 Stanley Hall, University of California, Berkeley, California 94720-3206

(RECEIVED August 14, 1998; ACCEPTED October 7, 1998)

Abstract

Electrostatic interactions are often critical for determining the specificity of protein-protein complexes. To study the role of electrostatic interactions for assembly of helical bundles, we previously designed a thermostable, heterotrimeric coiled coil, ABC, in which charged residues were employed to drive preferential association of three distinct, 34-residue helices. To investigate the basis for heterotrimer specificity, we have used multiwavelength anomalous diffraction (MAD) analysis to determine the 1.8 Å resolution crystal structure of ABC. The structure shows that ABC forms a heterotrimeric coiled coil with the intended arrangement of parallel chains. Over half of the ion pairs engineered to restrict helix associations were apparent in the experimental electron density map. As seen in other trimeric coiled coils, ABC displays acute knobs-into-holes packing and a buried anion coordinated by core polar amino acids. These interactions validate the design strategy and illustrate how packing and polar contacts determine structural uniqueness.

Keywords: electrostatic interactions; heterospecificity; heterotrimer; protein design; protein–protein interactions

Protein–protein interactions are critical for almost all biological functions. Mutational studies and atomic resolution structures of protein complexes indicate that they are stabilized by the full range of hydrophobic and polar contacts, including coordination of interfacial ions. These forces promote protein complexes that are both stable and specific, but it remains to be understood how interactions are restricted to particular partners. Understanding the determinants of specificity and stability has been difficult due to the complexity of most protein–protein interfaces.

An especially simple oligomeric structure in which interfacial interactions can be isolated and dissected is provided by the α-helical coiled coil (Cohen & Parry, 1994). Coiled coil motifs are found in a wide variety of proteins including intermediate filaments, cell surface receptors, molecular motors, and transcription factors. In most of these settings, coiled coils serve as molecular connectors, bringing together two or more protein modules, or as long fibers with varied biological activities. These diverse functions are accomplished by a simple fold in which two or more α-helices wrap around one another to form a supercoiled structure.

The supercoiling arises from a characteristic heptad repeat sequence, $(\mathbf{a}\,\mathbf{b}\,\mathbf{c}\,\mathbf{d}\,\mathbf{e}\,\mathbf{f}\,\mathbf{g})_n$ in which amino acids at positions **a** and **d** are typically hydrophobic, side chains at **e** and **g** are often charged and those at the solvent-exposed **b**, **c**, and **f** positions are predominantly polar. Residues at the **a** and **d** positions define the hydrophobic interface between helices and are critical for determining the oligomerization states of coiled coils (Harbury et al., 1993; Gonzalez et al., 1996a, 1996b). On the edge of the interface, interhelical ionic interactions can occur between residues at the **g** position of one heptad, $\mathbf{g}_n$, and the **e** position in the next heptad of the adjacent helix, $\mathbf{e}'_{n+1}$ (McLachlan & Stewart, 1975; O'Shea et al., 1991).

These electrostatic interactions play a key role in association of both naturally-occurring and designed heterodimeric coiled coils. In the leucine zippers of the Fos and Jun nuclear oncogene products, for example, eight amino acids at **g** and **e** positions are sufficient to mediate preferential heterodimer formation (Schuermann et al., 1991; O'Shea et al., 1992). The unfavorable interhelical electrostatic interactions between acidic residues at **g** and **e** positions that destabilize the Fos homodimer are replaced by more complementary charge interactions in the Fos/Jun heterodimer. This rationale was adopted for the design of obligate heterodimeric coiled coils, including the Velcro peptides (O'Shea et al., 1993; Zhou et al., 1994b). In these dimers, two sequences with identical core and surface sequences were designed with either all lysines or all glutamic acids at the **g** and **e** positions. In the Velcro system, electrostatic repulsion in the homodimers that is relieved upon formation of the heterodimers was found to be the sole determinant for heterospecificity (O'Shea et al., 1993).

To test whether $\mathbf{g}_n$ to $\mathbf{e}'_{n+1}$ interactions also could drive heterospecificity in trimeric coiled coils, we previously designed and characterized ABC, a parallel heterotrimer with a counterclockwise arrangement of the A, B, and C helices when viewed from the amino terminus (Fig. 1) (Nautiyal et al., 1995). Trimer formation was specified by a common core sequence containing isoleucines

Reprint requests to: Tom Alber, Department of Molecular and Cell Biology, 229 Stanley Hall #3206, University of California, Berkeley, California 94720-3206; e-mail: tom@ucxray6.berkeley.edu.

Abbreviations: MAD, multiwavelength anomalous diffraction; RMSD, root-mean-square deviation.

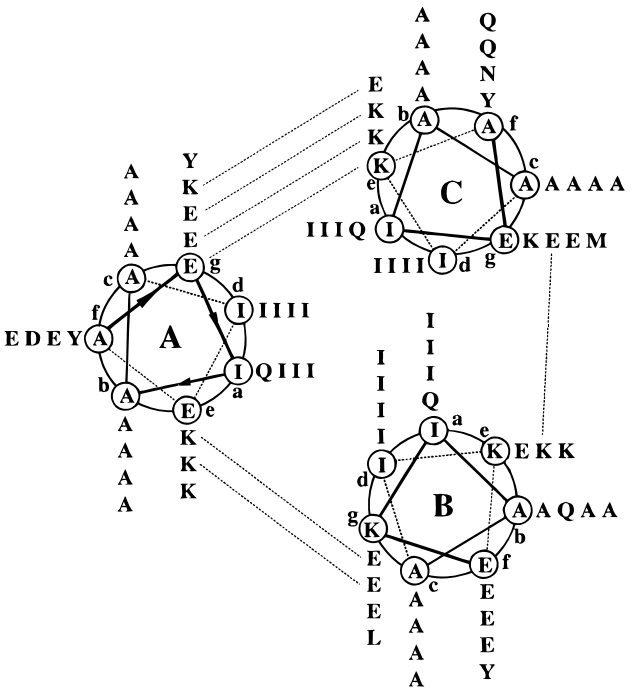

Fig. 1. Helical wheel representation of the ABC heterotrimer sequence. View is from the amino terminus with heptad positions labeled **a**–**g**. Each helix begins at an **f** position. The residue at the **g** position of each heptad can potentially form a salt bridge with the residue at the **e** position of the next heptad of an adjacent helix. The pattern of charge residues at the **g** and **e** positions maximizes complementary ion pairs in the counterclockwise, parallel heterotrimer. Dashed lines between helices indicate charged residues that are within ion-pairing distance in the crystal structure.

at the **a** and **d** positions (Harbury et al., 1993, 1994). A single **a**-position glutamine was introduced in each peptide to destabilize the system sufficiently to characterize under native conditions. A strategy of negative design was employed to favor the heterotrimer over alternate species, including homotrimers and antiparallel heterotrimers. The selected sequences were capable of forming 12 interhelical $\mathbf{g}_n - \mathbf{e}'_{n+1}$ ion pairs in the desired heterotrimer. Alternate trimeric species potentially contained at least four repulsive interactions and a maximum of eight complementary interactions. Solution studies indicated that A, B, and C preferentially associate with high specificity and stability. A mixture of 3.3 μM each of A, B, and C shows a highly cooperative thermal transition with a melting temperature of 87.5 °C. Furthermore, the heterotrimer showed an average thermal stabilization of 33 °C relative to the individual peptides and 21 °C relative to pairwise combinations of the peptides. ABC behaved as a single species when analyzed by anion exchange chromatography and native gel electrophoresis.

Although these studies indicated that A, B, and C interact in a specific manner, it remained unresolved whether the helices assembled as intended in the design. To investigate whether the interactions that formed the basis for the design occur in the heterotrimer, we have determined the high resolution crystal structure of ABC by multiwavelength anomalous diffraction (MAD) analysis. Compared to molecular replacement or conventional isomorphous replacement phasing methods, the MAD technique enabled a less biased evaluation of the high-resolution features of the structure, such as the ion pairs.

Results

Quality of the model

Data collected to 2.0 Å resolution at four wavelengths from a platinum derivative were used for MAD phasing (Table 1). The initial electron density map was improved by solvent flattening and histogram matching (CCP4, 1994). This procedure resulted in an exceptionally clear map (Fig. 2) in which most of the backbone and many of the side chains and solvent features could be traced unambiguously. An initial model built into the 2.0 Å resolution map was improved by subsequent rounds of rebuilding and refinement. The resolution was extended to 1.8 Å by refinement against data from a native crystal. The final model includes the entire main chain of each helix (102 amino acids and terminal capping groups), all but four side chains, 129 waters and one chloride ion. The model has a crystallographic *R*-factor of 20.8% and a free *R*-factor of 26.9% with excellent geometry (Table 1).

Overall structure

The A, B, and C chains associate to form a parallel, three-stranded coiled coil with the arrangement of helices expected from the design (Fig. 3). The core isoleucines exhibit acute knobs-into-

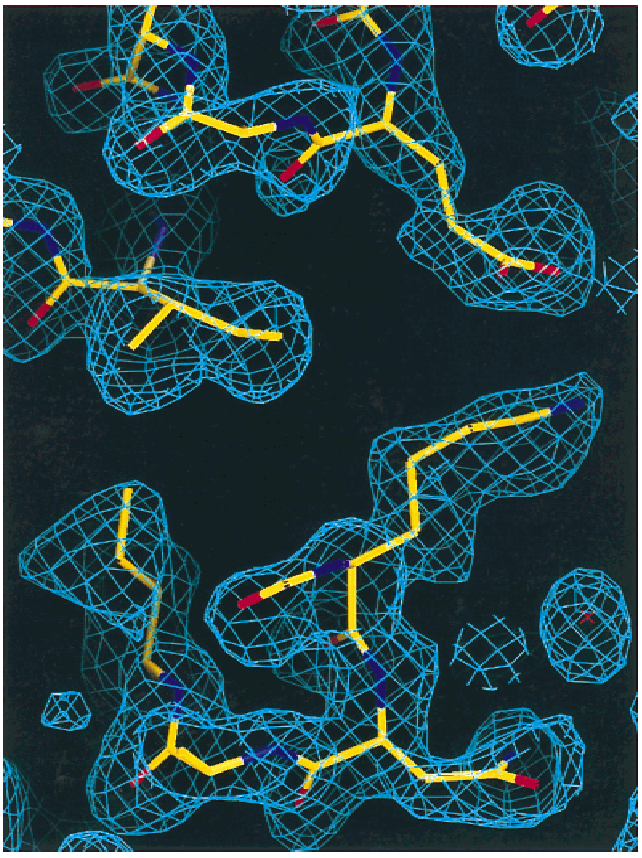

Fig. 2. Model superimposed on the experimental, 2.0-Å resolution electron density map calculated with solvent-flattened, MAD phases. Contour level is 1σ. The view shows the hydrogen-bonded ion pair between GluA9 and LysC14.

Table 1. *Data collection, phasing, and refinement statistics*

	Native	K_2PtCl_4
Space group	$P2_1$	$P2_1$
Unit cell dimensions		
a	21.93 Å	21.95 Å
b	35.01 Å	34.94 Å
c	66.46 Å	66.43 Å
β	93.70°	92.82°

Wavelength	Resolution (Å)	R_{merge}[a]	Completeness (%)	Multiplicity	$I/\sigma(I)$[b]	Phasing power[c] anomalous/dispersive
λ_1 (1.18077 Å)	25.0–2.0	0.037	99.1	9.3	14.8	0.64/1.13
λ_2 (1.07253 Å)	25.0–2.0	0.047	99.3	10.5	13.5	0.78/–
λ_3 (1.07194 Å)	25.0–2.0	0.043	99.2	8.4	11.5	1.01/0.73
λ_4 (1.00798 Å)	25.0–2.0	0.043	99.6	8.7	13.3	0.89/1.16
Native	25.0–1.8	0.036	99.2	3.8	14.2	

Mean figure of merit (25.0–2.0 Å)[d]: 0.63 (0.80 after solvent flattening)

Crystallographic R/R_{free} (6.0–1.8 Å)[e]: 0.208/0.269
RMS Δbonds, RMS Δangles[f]: 0.004, 0.636

[a] $R_{merge} = \Sigma|I - \langle I\rangle|/\Sigma I$; *I*, intensity.
[b] $I/\sigma(I)$; *I*, intensity.
[c] Phasing power = $[\Sigma_n|F_H|^2/\Sigma_n|E|^2]^{1/2}$; F_H, calculated heavy atom scattering factor; *E*, lack of closure error.
[d] Mean figure of merit = $\langle||\Sigma_\alpha P(\alpha)e^{i\alpha}/\Sigma_\alpha P(\alpha)||\rangle$; α, phase; $P(\alpha)$, phase probability distribution.
[e] $R_{cryst} = \Sigma|F_o - F_{calc}|/\Sigma F_o$; F_o, observed structure-factor amplitude; F_{calc}, calculated structure-factor amplitude.
[f] RMSDs from ideal values.

holes packing characteristic of trimeric coiled coils for almost the entire length of the trimer (Fig. 4A). Comparison of the first four heptads of ABC with the analogous region of GCN4-pII, a homotrimer with isoleucines at eight core positions (Harbury et al., 1994), yielded an RMSD of 0.85 Å for the main chains and equivalent core side chains. This correspondence suggests that the core glutamines and the substitution of more exposed residues cause little distortion of the superhelix.

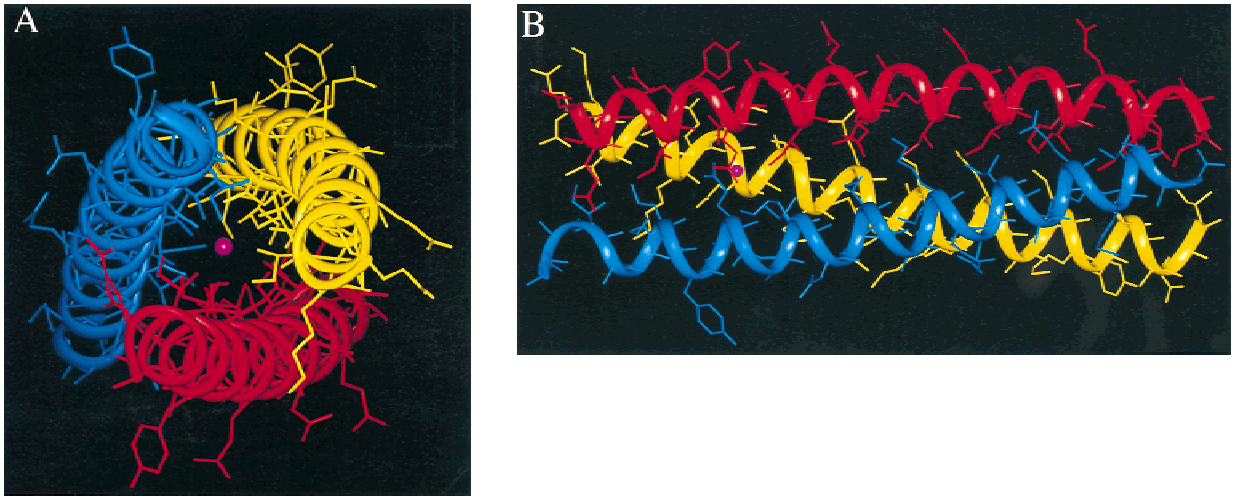

Fig. 3. Ribbon trace superimposed on a stick diagram of the ABC heterotrimer. The A helix is shown in red, the B in yellow, and the C in blue, and the chloride ion in magenta. **A:** View of the heterotrimer from the amino terminus down the superhelical axis. The chains have the designed, in-register, counterclockwise arrangement. The curvature of the helices is characteristic of coiled coils. Helix C straightens at the carboxy terminus due to local packing interactions. **B:** Side view showing the overall twist of the chains and the position of the buried chloride ion in the Gln10 layer.

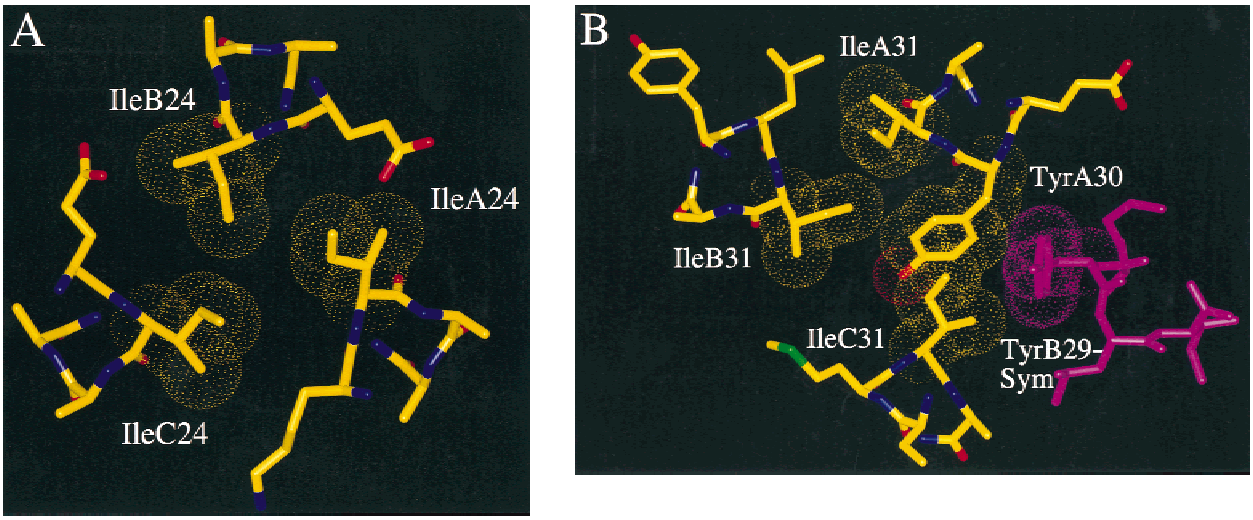

Fig. 4. Packing of core residues in ABC. **A:** Acute knobs-into-holes packing of core isoleucines in an **a** layer of the heterotrimer. **B:** Packing of TyrA30 into the hydrophobic core of the heterotrimer disrupts the conventional knobs-into-holes packing causing the C helix to splay. TyrB29 from a symmetry related molecule (magenta) packs against the interface of helix A and helix C.

Interhelical ion pairs

As judged by the distances between the charged atoms, 7 of the 12 engineered $\mathbf{g}_n - \mathbf{e}'_{n+1}$ complementary ion pairs are present in the final refined model (Table 2). The experimental electron density map calculated from the MAD analysis and solvent flattening clearly confirms five of these ion pairs and contains features consistent with the other two (Fig. 2). Electron density corresponding to the distal portion of LysC9, which is capable of pairing with GluB14, was not observed in any of the maps. Therefore, LysC9 was modeled as α-aminobutyric acid. Experimental electron density for the carboxylate group of GluC2 suggested that it participates in a solvent-mediated interaction with a neighboring trimer in the crystal, making GluC2 unavailable to pair with LysB7. Density for GluC2, however, was not apparent in the maps generated using model phases. Therefore, GluC2 was modeled as alanine. Based on the experimental electron density map, $\mathbf{g}_n - \mathbf{e}'_{n+1}$ ion pairs between LysB2 and GluA7 as well as GluB23 and LysA28 are clearly precluded by the conformations of these side chains. It is unclear why at least four of the ion pairs are not observed. The side chains in question are not involved in alternate $i + 3$ and $i + 4$ intrahelical interactions or in crystal packing contacts.

Table 2. *Atomic distances for interhelical ion pairs*

Ion pair	Distance (Å)
GluA2-LysC7	2.76
GluA9-LysC14	2.58
GluA16-LysC21	3.26
LysA23-GluC28	2.74
GluB9-LysA14	3.78
GluB16-LysA21	3.21
GluC16-LysB21	3.08

Core features

Refinement of the structure against the high resolution native data revealed a 12σ peak between the buried glutamines at the second **a** position of each helix. Based on the size of the peak and the components of the crystallization conditions, this electron density was modeled as a chloride ion (Fig. 5). The chloride ion is 3.3 Å away from the amide nitrogen of each glutamine. A stabilizing chloride ion bound by three buried asparagines was observed previously in a **d** layer in the structure of the transmembrane subunit of the envelope protein of Moloney murine leukemia virus (Mo-55) (Fass et al., 1996). In this case, the chloride ion was reported to be 3.25 Å away from the amide nitrogen of the asparagine. Chloride also was coordinated by glutamine at position **a** in the recently determined structure of GCN4-pIQ, a trimeric mutant of the GCN4 leucine zipper which has a pattern of core residues similar to ABC (Eckert et al., 1998). (Although no chloride was seen in the core of the GCN4 Asn16Gln trimer, the crystallization conditions lacked halide ions (Gonzalez et al., 1996b).) The buried chloride ions coordinated by polar groups in Mo-55, GCN4-pIQ, and ABC may be common structural features characteristic of trimeric coiled coils. In support of this idea, asparagine is found ~1.7 times more commonly at the **d** position in coiled-coil trimers than dimers, and strikingly, glutamine occurs ~11 times more frequently in the **a** position of trimers (Woolfson & Alber, 1995).

An unexpected feature observed in the crystal structure was the disruption of acute knobs-into-holes packing at the C-terminus of the heterotrimer. All three helices exhibit conventional coiled-coil geometries until position 29, at which point the C helix straightens. Inspection of the local side chain packing reveals that TyrA30, which occurs at a **g** position, packs into the trimer core (Fig. 4B). Based on its position within the heptad repeat, this tyrosine is expected to be only partially buried. It is possible that the placement of an extremely hydrophobic amino acid adjacent to an **a** position interrupts the characteristic 3,4 hydrophobic repeat of the coiled coil motif, thereby resulting in a structural irregularity. Alternatively, the straightening of the C helix may be the result of a

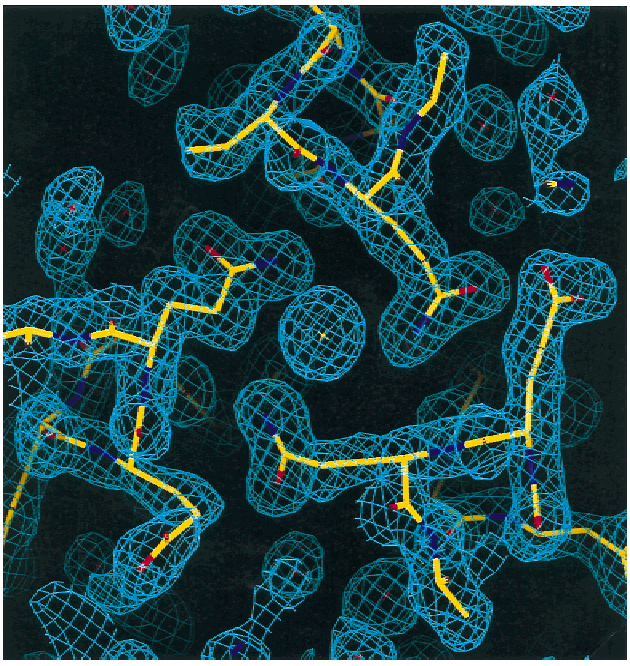

Fig. 5. A chloride ion is coordinated by three buried glutamines. The 6–1.8 Å resolution, $2F_o - F_c$ electron density map is shown superimposed on the model. The chloride ion is 3.3 Å from the amide nitrogen of each Gln10, located in the second **a** position of all three chains.

crystal packing contact from an adjacent trimer. TyrB29 from a symmetry mate packs against the interface of helices A and C (Fig. 4B), preventing TyrA30 from assuming a position which is more solvent exposed.

Discussion

Early attempts at *de novo* protein design, based largely on secondary structure propensities and binary patterning of hydrophobic and polar amino acids, often produced proteins with properties similar to those of molten globules (Betz et al., 1993). These polypeptides had the desired secondary structure but lacked specific tertiary interactions. This structural polymorphism suggested that minimalist strategies may be inadequate for imparting a unique fold. Introduction of specific tertiary interactions has recently led to the design of proteins with native-like properties (O'Shea et al., 1993; Betz et al., 1995, 1997; Bryson et al., 1995; Dahiyat & Mayo, 1997; Ogihara et al., 1997; Schafmeister et al., 1997; Harbury et al., 1998). Extensive studies on the structure, stability, and oligomerization of coiled coils have made this protein family an especially favorable design target. Our design strategy for ABC considered not only secondary-structure propensities and hydrophobic-polar patterning, but also core packing, buried polar interactions, and specific interhelical electrostatic interactions.

This design strategy is validated by the high resolution crystal structure of ABC. In contrast to previous coiled-coil structures that relied on model phases to obtain high-resolution electron density maps, a more direct view of ABC was obtained by MAD analysis at 2.0 Å resolution. The structure shows that the helices are oriented in the intended manner. In addition, ABC exhibits the expected acute knobs-into-holes packing, anion coordination by buried polar groups and ion pairs between residues at $\mathbf{g}_n$ and $\mathbf{e}'_{n+1}$ positions. Although examples of designed hetero-oligomeric coiled coils in which association is driven by electrostatic interactions have been reported (O'Shea et al., 1993; Zhou et al., 1994b; Olive et al., 1996; Sharma et al., 1998), the structures of these oligomers have not been determined. The MAD analysis of ABC provides new structural evidence for the occurrence of ion pairs engineered between Glu and Lys residues at $\mathbf{g}_n$ and $\mathbf{e}'_{n+1}$ positions, suggesting that these interactions are important for specificity.

While $\mathbf{g}_n - \mathbf{e}'_{n+1}$ interactions are clearly important for specificity, the stabilizing contribution of attractive ion pairs is controversial (Krylov et al., 1994, 1998; Zhou et al., 1994a; Lumb & Kim, 1995; Lavigne et al., 1996). In dimeric coiled coils, studies employing double mutant cycles have suggested that ion pairs between glutamic acids and lysines can contribute -0.1 to -0.9 kcal/mol to the stability of a dimeric coiled coil (Krylov et al., 1994, 1998; Zhou et al., 1994a). In contrast, measurement of the pK_a's of glutamates in the GCN4 leucine zipper positioned to participate in $\mathbf{g}_n - \mathbf{e}'_{n+1}$ salt bridges indicated that the net energetic contribution of electrostatic interactions between ionized glutamic acid with the rest of the protein was 0 to $+0.3$ kcal/mol (Lumb & Kim, 1995). Thermodynamic studies of the Fos/Jun heterodimers (O'Shea et al., 1992) and the designed Velcro heterodimers (O'Shea et al., 1993) suggested that attractive ion pairs do not contribute to stability. Consensus exists, however, that repulsive ion pairs of homodimeric coiled coils are destabilizing, and relieving these unfavorable interhelical interactions can serve as a major driving force for heterodimer formation.

Although no comparable studies on the energetic contribution of electrostatic interactions have been carried out for trimeric coiled coils, our data demonstrate that residues at **g** and **e** positions are critical for determining specificity. Because A, B, and C have common core residues, their preferential association must be mediated by the pattern of charged residues at **g** and **e**. The charge pattern discriminates against a significant number of alternate species including a clockwise heterotrimer and all combinations of one or two chains. The $\mathbf{g}_n - \mathbf{e}'_{n+1}$ ion pairs in ABC are generally shorter than equivalent interactions observed in the crystal structure of the GCN4 dimer, suggesting that complementary ion pairs may make different energetic contributions in trimers and dimers.

The idea that interhelical ion pairs can help mediate assembly of trimers was proposed previously based on analysis of charged residues in the heterotrimeric coiled-coil laminin proteins (Beck et al., 1993; Kammerer et al., 1995). The positions of charged residues in the laminin sequences are consistent with a central role for complementary ion pairs that are formed only in the heterotrimer. Solution studies indicate that the $\beta 1$ and $\gamma 1$ chains of mouse laminins form a heterodimer containing a potentially destabilizing acidic pocket at one of the interfaces (Nomizu et al., 1996). Association of this dimer with a basic region of the $\alpha 2$ chain most likely relieves repulsive interactions resulting in the formation of a stable triple stranded coiled coil. Thus, principles that were used to guide the design of ABC may also underlie specificity of associations in naturally occurring heterotrimeric coiled coils.

Materials and methods

Crystallization

Peptides (A: Acetyl-A-E-I-A-A-I-E-Y-E-Q-A-A-I-K-E-E-I-A-A-I-K-D-K-I-A-A-I-K-E-Y-I-A-A-I-Amide, B: Acetyl-E-K-I-A-A-I-

K-E-E-Q-A-A-I-E-E-E-I-Q-A-I-K-E-E-I-A-A-I-K-Y-L-I-A-Q-I-Amide, and C: Acetyl-A-E-I-A-A-I-K-Y-K-Q-A-A-I-K-N-E-I-A-A-I-K-Q-E-I-A-A-I-E-Q-M-I-A-A-I-Amide) were synthesized and purified as described previously (Nautiyal et al., 1995). The heterotrimer was prepared by mixing approximately equimolar amounts of the individual peptides to a final peptide concentration of 250 μM. The mixture was subjected to high resolution ion-exchange chromatography on a Vydac 301VHP552 anion-exchange column using a linear gradient of 0 M to 0.5 M NaCl with 20 mM Tris pH 7.3 as the buffer. The major peaks from several runs were collected, pooled, and dialyzed against 10 mM Tris-HCl, pH 7.3. The dialyzed sample was lyophilized and subsequently dissolved in a small volume of H_2O. The concentrated sample was diluted to a final peptide concentration of 200 μM in 6 M urea, allowed to equilibrate for 45 min and dialyzed against 20 mM Tris-HCl pH 7.3 for >36 h. The dialyzed mixtures were re-chromatographed using ion-exchange chromatography as described above. The major peak was collected, dialyzed against 10 mM potassium phosphate pH 7.1 and lyophilized. The protein was dissolved in H_2O to a final concentration of 10 mg/mL for crystallization. Crystals were grown by vapor diffusion from 100 mM Tris-HCl pH 7.5, 50 mM $MgCl_2$, and 25% PEG 4000. The crystals had $P2_1$ symmetry (a = 21.93, b = 35.01, c = 66.46, b = 93.70) with one heterotrimer in the asymmetric unit.

Data collection, phase determination, and refinement

Crystals were briefly transferred to 50% PEG 4000 and flash frozen in liquid nitrogen for data collection. Native data were collected to 1.8 Å resolution on an R-Axis II image plate detector mounted on a Rigaku RU200 rotating anode generator.

Phase determination was by the multiwavelength anomalous diffraction (MAD) technique. A Pt^{2+} derivative was obtained by soaking the crystals overnight in 100 mM Tris-HCl pH 7.5, 50 mM $MgCl_2$, 25% PEG 4000, and 2 mM K_2PtCl_4. Crystals were then back soaked for at least 30 min in cryoprotectant and frozen. MAD data were collected from a single crystal on Fuji image plates at SSRL beam line 1–5 using inverse-beam geometry to measure Friedel pairs. Wavelengths were chosen at two remote points, λ_1 (1.18007 Å) and λ_4 (1.00798 Å), above and below the platinum absorption edge, respectively, the absorption edge inflection point λ_2 (1.07253 Å), and the peak λ_3 (1.07194 Å). Data were integrated using DENZO (Otwinowski & Minor, 1996) and scaled with SCALA from the CCP4 Suite (CCP4, 1994). Dispersive difference and anomalous difference Patterson maps, respectively, revealed a common 15σ peak and a 16σ peak that were consistent with a single platinum site. Experimental phases were calculated with MLPHARE (CCP4, 1994) using both dispersive and anomalous differences to 2.0 Å resolution. λ_2 was used as the reference wavelength. The experimental map was further improved using DM for solvent flattening and histogram matching. This yielded a clear electron density that could be traced unambiguously.

The model was built using the program O (Jones et al., 1991) and refined with X-PLOR (Brünger, 1993). A test set containing 10% of the reflections was used for calculation of the free *R*-factor. The first two rounds of refinement were done using experimental phases and subsequent rounds were done using model phases. The model was initially refined using data collected at λ_1. To obtain the structure of the heterotrimer free of the heavy atom and to extend the resolution to 1.8 Å, data collected on a native crystal were used for the final refinement. After placing the model in the unit cell of the native crystal, the individual helices and individual heptads were subjected to rigid body refinement to determine whether any backbone rearrangements had occurred. Torsional refinement was carried out and omit maps were generated for the entire molecule, 11 amino acids at a time, to check for changes in side-chain rotamers. Subsequent refinement steps included cycles of manual rebuilding, positional refinement, and individual *B*-factor adjustments.

The present model includes a complete backbone for each helix (including N-terminal acetyl caps and C-terminal amino caps), all side chains except C3 and C35, which are modeled as alanines, and C10 and C30, which are modeled as α-aminobutyric acid, 129 waters, and 1 chloride. A bulk solvent correction was applied after the final round of refinement. Analysis of model geometry with PROCHECK (CCP4, 1994) revealed no Ramachandran violations and most side chains in common rotamers. Atomic coordinates (ID 1BB1) are available from the Brookhaven Protein Data Bank.

Acknowledgments

We thank David S. King and Robert Schackmann for peptide synthesis; members of the Alber lab, the Nelson lab, and Henry Bellamy at SSRL for assistance with data collection; and Otis Littlefield for advice on MAD phasing. We also thank Ed Rebar, Pehr Harbury, Bob Matthews, and Peter Kim for critical reading of the manuscript. X-ray data were collected at SSRL, which is operated by the Department of Energy, Office of Basic Energy Sciences. The SSRL Biotechnology Program is supported by the National Institutes of Health, National Center for Research Resources, Biomedical Technology Program, and by the Department of Energy, Office of Biological and Environmental Research. This work was supported by NIH grant GM48958 to T.A. and a NSF Multi-user Biological Equipment award.

References

Beck K, Dixon TW, Engel J, Parry DA. 1993. Ionic interactions in the coiled-coil domain of laminin determine the specificity of chain assembly. *J Mol Biol 231*:311–323.

Betz SF, Bryson JW, DeGrado WF. 1995. Native-like and structurally characterized designed alpha-helical bundles. *Curr Opin Struct Biol 5*:457–463.

Betz SF, Liebman PA, DeGrado WF. 1997. *De novo* design of native proteins: Characterization of proteins intended to fold into antiparallel, rop-like, four-helix bundles. *Biochemistry 36*:2450–2458.

Betz SF, Raleigh DP, DeGrado WF. 1993. De novo protein design: From molten globules to native-like states. *Curr Opin Struct Biol 3*:601–610.

Brünger AT. 1993. *XPLOR: A system for X-ray crystallography and NMR*. New Haven: Yale University Press.

Bryson JW, Betz SF, Lu HS, Suich DJ, Zhou HX, O'Neil KT, DeGrado WF. 1995. Protein design: A hierarchic approach. *Science 270*:935–941.

CCP4. 1994. The CCP4 Suite: Programs for protein crystallography. *Acta Cryst D50*:760–763.

Cohen C, Parry DAD. 1994. α-Helical coiled coils: More facts and better predictions. *Science 263*:488–489.

Dahiyat BI, Mayo SL. 1997. *De novo* protein design: Fully automated sequence selection. *Science 278*:82–87.

Eckert DM, Malashkevich VN, Kim PS. 1998. Crystal structure of GCN4-pIQ, A trimeric coiled coil with buried polar residues. *J Mol Biol*. Forthcoming.

Fass D, Harrison SC, Kim PS. 1996. Retrovirus envelope domain at 1.7 angstrom resolution. *Nat Struct Biol 3*:465–469.

Gonzalez L Jr, Brown RA, Richardson D, Alber T. 1996a. Crystal structures of a single coiled-coil peptide in two oligomeric states reveal the basis for structural polymorphism. *Nat Struct Biol 3*:1002–1009.

Gonzalez L Jr, Woolfson DN, Alber T. 1996b. Buried polar residues and structural specificity in the GCN4 leucine zipper. *Nat Struct Biol 3*:1011–1018.

Harbury PB, Kim PS, Alber T. 1994. Crystal structure of an isoleucine-zipper trimer. *Nature 371*:80–83.

Harbury PB, Plecs JJ, Tidor B, Alber T, Kim PS. 1998. High resolution protein design with backbone freedom. *Science 282*:1462–1467.

Harbury PB, Zhang T, Kim PS, Alber T. 1993. A switch between two-, three-, and four-stranded coiled coils in GCN4 leucine zipper mutants. *Science 262*:1401–1407.

Jones TA, Zou JY, Cowan SW, Kjeldgaard M. 1991. Improved methods for the building of protein models in electron density maps and the location of errors in these models. *Acta Cryst A47*:110–119.

Kammerer RA, Antonsson P, Schulthess T, Fauser C, Engel J. 1995. Selective chain recognition in the C-terminal α-helical coiled-coil region of laminin. *J Mol Biol 250*:64–73.

Krylov D, Barchi J, Vinson C. 1998. Inter-helical interactions in the leucine zipper coiled coil dimer: pH and salt dependence of coupling energy between charged amino acids. *J Mol Biol 279*:959–972.

Krylov D, Mikhailenko I, Vinson C. 1994. A thermodynamic scale for leucine zipper stability and dimerization specificity: e and g interhelical interactions. *EMBO J 13*:2849–2861.

Lavigne P, Sonnichsen FD, Kay CM, Hodges RS. 1996. Interhelical salt bridges, coiled-coil stability, and specificity of dimerization. *Science 271*:1136–1138.

Lumb KJ, Kim PS. 1995. Measurement of interhelical electrostatic interactions in the GCN4 leucine zipper. *Science 268*:436–439.

McLachlan AD, Stewart M. 1975. Tropomyosin coiled-coil interactions: Evidence for an unstaggered structure. *J Mol Biol 98*:293–304.

Nautiyal S, Woolfson DN, King DS, Alber T. 1995. A designed heterotrimeric coiled coil. *Biochemistry 34*:11645–11651.

Nomizu M, Utani A, Beck K, Otaka A, Roller PP, Yamada Y. 1996. Mechanism of laminin chain assembly into a triple-stranded coiled-coil structure. *Biochemistry 35*:2885–2893.

Olive M, Williams SC, Dezan C, Johnson PF, Vinson C. 1996. Design of a C/EBP-specific, dominant-negative bZIP protein with both inhibitory and gain-of-function properties. *J Biol Chem 271*:2040–2047.

Ogihara NL, Weiss MS, Degrado WF, Eisenberg D. 1997. The crystal structure of the designed trimeric coiled coil coil-VaLd: Implications for engineering crystals and supramolecular assemblies. *Protein Sci 6*:80–88.

O'Shea EK, Klemm JD, Kim PS, Alber T. 1991. X-ray structure of the GCN4 leucine zipper, a two-stranded, parallel coiled coil. *Science 254*:539–544.

O'Shea EK, Lumb KJ, Kim PS. 1993. Peptide 'Velcro': Design of a heterodimeric coiled coil. *Curr Biol 3*:658–667.

O'Shea EK, Rutkowski R, Kim PS. 1992. Mechanism of specificity in the Fos-Jun oncoprotein heterodimer. *Cell 68*:699–708.

Otwinowski Z, Minor W. 1996. Processing of X-ray diffraction data collected in oscillation mode. *Methods Enzymol 276*:307–326.

Schafmeister CE, LaPorte SL, Miercke LJ, Stroud RM. 1997. A designed four helix bundle protein with native-like structure. *Nat Struct Biol 4*:1039–1046.

Schuermann M, Hunter JB, Hennig G, Muller R. 1991. Non-leucine residues in the leucine repeats of Fos and Jun contribute to the stability and determine the specificity of dimerization. *Nucleic Acids Res 19*:739–746.

Sharma VA, Logan J, King DS, White R, Alber T. 1998. Sequence-based design of a peptide probe for the APC tumor suppressor protein. *Curr Biol 8*:823–830.

Woolfson DN, Alber T. 1995. Predicting oligomerization states of coiled coils. *Protein Sci 4*:1596–1607.

Zhou NE, Kay CM, Hodges RS. 1994a. The net energetic contribution of interhelical electrostatic attractions to coiled-coil stability. *Protein Eng 7*:1365–1372.

Zhou NE, Kay CM, Hodges RS. 1994b. The role of interhelical ionic interactions in controlling protein folding and stability. *De novo* designed synthetic two-stranded alpha-helical coiled-coils. *J Mol Biol 237*:500–512.